Journal of Circuits, Systems, and Computers, Vol. 7, No. 3 (1997) 153–164

PULSED CHARGE MODEL OF FAULT BEHAVIOR PRODUCING SEISMIC ELECTRIC SIGNALS (SES)*

MOTOJI IKEYA, SHUNJI TAKAKI, HIROSHI MATSUMOTO,
ATSUSHI TANI, and TAKAHIDE KOMATSU
Department of Earth and Space Sciences, Graduate School of Science
Osaka University, 1-1 Machikaneyama Toyonaka, Osaka 560, Japan
E-mail: ikeya@ess.sci.osaka-u.ac.jp

Received 23 December 1996
Revised 13 February 1997
Accepted 2 April 1997

The electromagnetic (EM) behavior of a geological fault is postulated to follow the mathematical model of a fault in seismology that illustrates seismic EM anomalies (EMAs). Charge densities, $+q$ and $-q$ in C/m^2 are generated at a fault zone by the change in seismic stress, σ as $\mathrm{d}q/\mathrm{d}t = -\alpha \mathrm{d}\sigma/\mathrm{d}t - q/\varepsilon\rho$, where σ, ε and ρ are the charge generation constants measured in C/N, dielectric constant and resistivity of bedrocks, respectively. A fault of length, $2a$, plane area, A and the displacement or rupture time, τ gives pulsed charge densities, $+q(t)$ and $-q(t)$, or a dipole moment of $P(t) = 2aAq(t) = \alpha M_0[\varepsilon\rho/(\tau - \varepsilon\rho)][\exp(-t/\tau) - \exp(-t/\varepsilon\rho)]$ using the earthquake moment M_0. Maxwell's equations for this dipole in a conductive earth give power spectra of EM waves at different distances. Seismic electric signals (SES) including the DC VAN method can be explained as EM waves. Electrons with density n in the atmosphere are accelerated by the electric field and travel a distance l, resulting in the excitation and ionization of atmospheric molecules leading to earthquake lightning (EQL). They also polarize the ionosphere by disturbing the transmission of EM waves. Preliminary results of pulsed electric field measurements are presented for lightning, prior to an earthquake and artificial electronic noises. The same pulsed field surprised eels and hamsters, suggesting seismic anomalous animal behavior (SAAB) as electro-physiological responses to the stimuli of electric pulses.

1. Introduction

Earthquake lightning (EQL), seismic anomalous animal behavior (SAAB) and electromagnetic anomaly (EMA) were observed prior to or at the time of the Kobe Earthquake on January 17 1995, as published in a book in which retrospectively collected statements from citizens are collected.[1] These phenomena have provoked interest in popular science and in the press, but scientific interest has been limited.

The retrospective approach may be a first step in the documentation of precursor phenomena. However, data all over the world ended up simply as records and so is currently beyond our interpretation. A phenomenon must be explained with

*This letter was recommended by Associate Editor I. Shirakawa.

a hypothesis or a model and then by a theory. A clear model to explain these phenomena is so far not available. We have proposed an electromagnetic (EM) model of fault behavior and explained EQL[2] as seismo-atmospheric luminescence and SAAB as animals' electro-physiological response.[3]

Most EMA reported as noises in radio and TV broadcasting were suspected to be due to seismic EM waves at different frequencies and also to disturbances of the ionosphere which reflect radiowaves. Although seismologists are skeptical, efforts to clarify the phenomena and to predict earthquakes are being made by telecommunication engineers.[4,5] In this paper, we report that pulsed charges caused by preseismic and coseismic stress changes can explain EMA by solving Maxwell's equations for the time-dependent electric dipole moment, related to the earthquake moment.

2. An Electromagnetic Model of a Fault

2.1. *A mathematical model of a fault*

A mathematical model of a fault has been used in seismology.[6,7] A fault having a fault plane with area, A, length, $2a$, final displacement, D and rigidity of the rock, μ, gives the earthquake moment, M_0 as $M_0 = \mu DA$. The time-dependent displacement, $D(t)$ is expressed using the initial displacement velocity, D', as

$$D(t) = D[1 - \exp(-D't/D)]\,. \tag{1}$$

The displacement time, $\tau = D/D'$, is described using $D = 2\Delta\sigma a/\mu$ and $D' = 2\sigma_0\beta/\mu$ as

$$\tau = D/D' = (\Delta\sigma/\sigma_0)(a/\beta)\,, \tag{2}$$

where $\sigma_0, \Delta\sigma$ and β are the stress before faulting, the stress drop by the displacement and the velocity of secondary waves ($3.5 \sim 4$ km/s), respectively. The time-dependent stress, $\sigma(t) = \mu[D - D(t)]/2a$, gives

$$\sigma(t) = \Delta\sigma \exp(-t/\tau)\,. \tag{3}$$

The stress distribution at a fault zone is not simple[6] but may be roughly described as shown in Fig. 1(a). The stress area may be approximated as an area of length $2a$ and width $2a$ as in Fig. 1(b). Inhomogeneous movement of the fault resulting in the deterministically chaotic movement may also be described using Eq. (3) for τ of the order of μs.[8,9]

2.2. *An electromagnetic model of fault behavior*

2.2.1. *Separated charges with a decay constant of* $\varepsilon\rho$

In this model, a fault is described as a capacitor with capacitance, C and leak resistance, R, having a resistivity ρ and a dielectric constant $\varepsilon(\varepsilon^* = \varepsilon/\varepsilon_0 = 8)$ of the earth. For a plate capacitor with area A and separation $2a$, $C = \varepsilon A/2a$

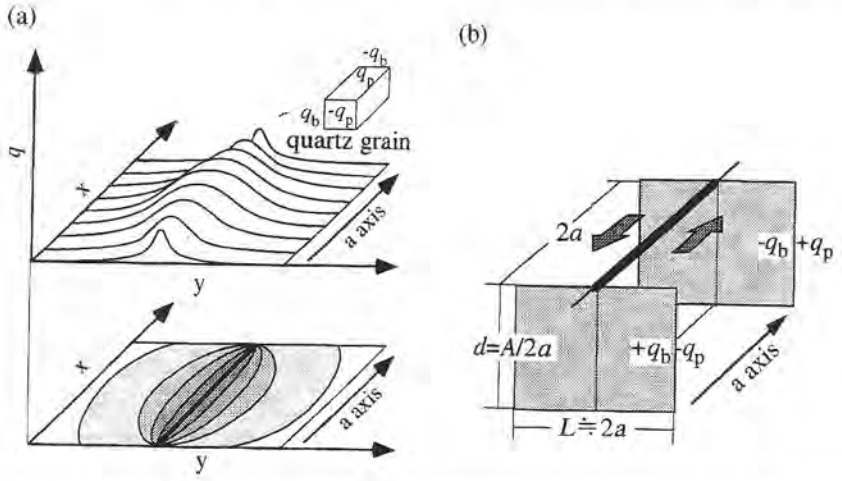

Fig. 1. (a) A model of a fault with a seismic stress distribution. The magnitude of stress is highly released in the dark area, and the bound charge appears in proportion to stress drop after the stress release. No apparent charge is present as $q_b - q_p = 0$. (b) A simplified model of a fault having uniform stress distribution. Transient dipolar charge densities of $+q(t)$ and $-q(t)$, where $q(t) = q_b(t) - q_p(t)$ appears as a result of the change in seismic stress.

and $R = 2\rho a/A$, and so $CR = \varepsilon\rho$. A capacitor of two parallel infinite lines with the separation $2a$ leads also to $CR = \varepsilon\rho$. Equations $\mathrm{d}Q/\mathrm{d}t = -I = -V/R$ and $V = Q/C$ give $\mathrm{d}Q/\mathrm{d}t = -Q/CR$ leading to $Q = Q_0 \exp(-t/\varepsilon\rho)$.

The decay time or charge sustention time, $\varepsilon\rho$, ranges from 7 ns for sediments ($\rho = 10^2$ Ωm) to 70 μs for igneous rocks ($\rho = 10^6$ Ωm). Lockner *et al.*[10] proposed that $\rho = 10^6$ Ωm for granite increases to $\rho = 10^{10}$ Ωm as a result of the evaporation of water during faulting, leading to $\varepsilon\rho = 1$ s though the asserted thermal diffusion of the frictional heat is somewhat questionable.

2.2.2. *A mechanism: piezo-compensating bound charges*

Electric charge densities, q_b, known as "bound charges" (actually free charges) cancel the stress-induced piezoelectric polarization having the surface density of q_p in the conductive earth. Neither free charge nor electric field is present at the fault zone since the seismic stress has accumulated gradually to be $q_p - q_b = 0$. However, the charge densities $+q(t)$ and $-q(t)$, where $q(t) = q_b(t) - q_p(t)$, appear transiently when seismic stress is changed, either by faulting (main shock) or by local fractures of rocks (foreshocks). Suppose $q_p(t) = \alpha\sigma(t)$ neglecting the tensor properties of the piezoelectric coefficient, α.[11] Both densities, q_p and q_b, change as

$$\mathrm{d}q_p/\mathrm{d}t = \alpha\,\mathrm{d}\sigma/\mathrm{d}t\,, \tag{4}$$

$$\mathrm{d}q_b/\mathrm{d}t = -(q_b - q_p)/\varepsilon\rho\,. \tag{5}$$

Hence, $q(t) = q_b(t) - q_b(t)$ is, by subtracting Eq. (4) from Eq. (5),

$$\mathrm{d}q/\mathrm{d}t = -\alpha(\mathrm{d}\sigma/\mathrm{d}t) - q/\varepsilon\rho\,. \tag{6}$$

From Eq. (3), Eq. (6) is given as $\mathrm{d}q/\mathrm{d}t = \alpha(\Delta\sigma/\tau)\exp(-t/\tau) - q/\varepsilon\rho$. The condition $q = 0$ at $t = 0$ gives

$$q(t) = \alpha\Delta\sigma[\varepsilon\rho/(\tau - \varepsilon\rho)][\exp(-t/\tau) - \exp(-t/\varepsilon\rho)]\,. \tag{7}$$

The piezoelectricity in quartz bearing rocks may arise from orientation inhomogeneity due to the preferential orientation of crystalline axes. The orientational anisotropy was observed for pyroxene and olivine from the difference of the propagation speed of seismic P- and S-waves. Our experiments on granite indicate that α is about 1%–0.01% of the piezoelectric coefficient of a quartz in agreement with those reported by Volarovich and Sobolev.[12] Any mechanism other than piezoelectricity[13] is plausible in this model so long as charges are generated by the change of stress as in Eq. (6) in the following arguments.

2.2.3. *The area of the charge appearance*

If an orientational anisotropy is present, for instance, along the fault direction, the charge appears on both sides of the stressed area as a result of an ensemble of polarization dipoles. Figure 1(a) shows the stress distribution at a fault zone. The piezo-compensating charges appear transiently following Eq. (7).

The charge distribution may be approximated for a constant seismic stress with width $2a$ and depth $A/2a$ leading to $Q = Aq$ as in Fig. 1(b). The dipole moment is described as $P = 2aQ = 2aAq = (M_0/\Delta\sigma)q$ using the moment $M_0 = \mu D A = 2aA\Delta\sigma$. The moment magnitude, M_W, is defined as $M_\mathrm{W} = (\log M_0 - 9.1)/1.5$ in seismology. Thus, the transient electric dipole moment at an epicenter is correlated with the seismic moment.

2.2.4. *Microscopic basis of charge separation to fault edges*

Orientational anisotropy of quartz grains is not necessarily needed in this microscopic consideration. The total energy of the emitted electromagnetic waves is proportional to the square of the total electric dipole moment at the fault zone, P which is the vector sum of the small dipole p_i as $P = \Sigma p_i$. Freed piezo-compensating charges around quartz grains constitute electric dipoles with the dipole moment p_i; the total energy is $P^2 = \Sigma p_i^2 = np^2$ for the same dipoles of $p_i = p$ and the total number of the small dipoles n. Hence, $P = n^{1/2}p$.

The number of the dipole moment is $n = 2aA\eta/(2a')^3$ considering the volume fraction η of simultaneously broken quartz with the grain length of $2a'$; accurately, η is a volume fraction of quartz grains whose electromagnetic waves are detected simultaneously at the observed point at the distance R. The dipole moment $p = (2a')^3 q(t)$. Hence the total dipole moment is $P = n^{1/2}p = [2aA\eta(2a')^3]^{1/2}q(t)$. One

may consider a large amount of charges appearing at both ends of the fault edge separated by a distance of $2a$ with the charges $Q = P/2a = [2aA\eta(2a')^3]^{1/2}q(t)/2a$. This is the microscopic basis of our electromagnetic model of fault behavior. One might consider an effective piezoelectric coefficient, $\alpha_{\text{eff}} = [(A\eta/2a)(2a')^3]^{1/2}\alpha$, for the fault zone. Preseismic phenomena may be discussed for a local fault segment of small $2a$ and A.

2.3. *Charge generation by seismic stress changes*

2.3.1. *A model of charge generation*

The first term on the right side of Eq. (6) is the generation of charges, the second term is the decay through earth and atmosphere with the effective $\rho^*(1/\rho^* = 1/\rho + 1/\rho_{\text{atm}})$; the resistivity of the atmosphere is neglected and $\rho^* = \rho$ is assumed. Total polarization is $P(t) = 2aAq(t)$ using the earthquake moment M_0 as

$$P(t) = \alpha M_0[\varepsilon\rho/(\tau - \varepsilon\rho)][\exp(-t/\tau) - \exp(-t/\varepsilon\rho)]\,. \tag{8}$$

2.3.2. *Coseismic and preseismic charge densities*

(a) On an Earthquake: coseismic electric field

The fault displacement time, $\tau = 1.7$ s is obtained from Eq. (2) for $2a = 12$ km and $\beta = 3.5$ km on the Nojima Fault and for 100% stress drop, $\Delta\sigma/\sigma_0 = 1$. Charges persist for faulting as $q(t) = \alpha\Delta\sigma(\varepsilon\rho/\tau)\exp(-t/\tau)$ for $\tau \gg \varepsilon\rho$ as indicated in Fig. 2(a). If one uses $\alpha = 10^{-14}$ C/N and $\sigma_0 = \Delta\sigma = 10^8$ N/m^2 for granite ($\varepsilon^* = 8$ and $\rho = 10^6$ Ωm: $\varepsilon\rho = 7 \times 10^{-5}$ s), the density, $q = 4 \times 10^{-11}$ C/m^2, gives

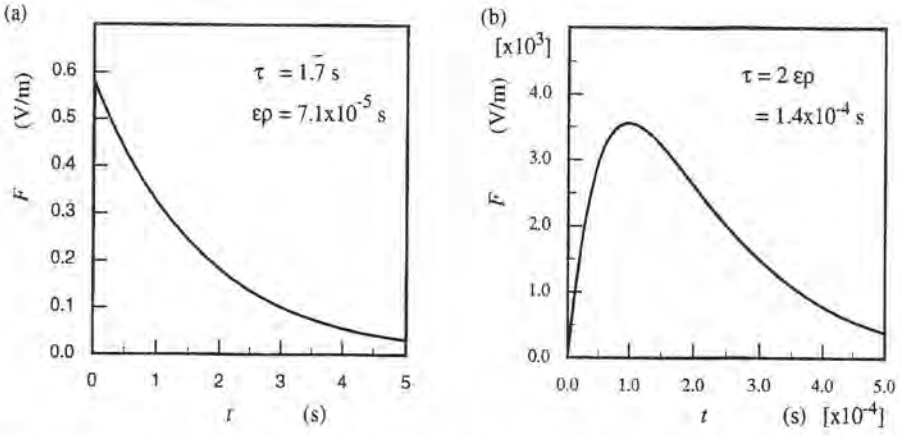

Fig. 2. The time-dependent electric field intensity due to seismic stress change in granitic bedrocks with $\rho = 10^6$ Ωm ($\varepsilon\rho = 7 \times 10^{-5}$s) for (a) the displacement time of $\tau = 1.7$ s (earthquake), (b) local fracture for a case of $\tau = 2\varepsilon\rho = 1.4 \times 10^{-4}$s (foreshock). Note that the intensity is four orders of the magnitude higher for preseismic (b) than coseismic (a).

the field intensity $F = q/\varepsilon^*\varepsilon_0 = 0.6$ V/m at the epicenter; the intensity is too low to cause EQL.[2]

If ρ becomes as high as 10^9 Ωm at the time of a major shock due to fractures of rocks by foreshocks, or to dilatancy before water fill in the porocity of the rock, the initial charge density becomes $q(0) = 10^{-5}$ C/m^2 due to the long time duration of $\varepsilon\rho = 0.1$ s: Unless ρ is enhanced, the resultant $q(0) = 10^{-8}$ is too small to cause coseismic anomalies for a homogeneous displacement of a fault.[14]

(b) Local fractures of rocks as precursors: preseismic electric field

An abrupt stress change due to the displacement of a fault segment with length $2a'$ gives large charge densities for inhomogeneous faulting. A burst of pulses of $q(t) = \alpha\sigma_0(\beta/a')$ with a short τ is expected.[3] No orientational anisotropy is needed since dipoles appear successively; some may cancel out but others may add up resulting in an ensemble average within the fluctuation.

Local fractures release the stress of a fault segment. An extreme case is the virtual fault length of the diameter of quartz grains ($2a = 7$ mm for example). The complete local stress drop, i.e. $\Delta\sigma/\sigma_0 = 1$, leads to $\tau = 10^{-6}$ s comparable to $\varepsilon\rho$. Figure 2(b) shows a case for $\tau = 2\varepsilon\rho = 1.4 \times 10^{-4}$ s for granite fracture. Note that the peak height is much higher than in Fig. 2(a) suggesting why some precursor phenomena are preseismic.

3. Electromagnetic Anomalies (EMAs)

3.1. *Generation of electromagnetic (EM) waves*

3.1.1. *Maxwell's equations for time-dependent seismic dipoles*

The telecommunication equation in Lorentz gauge for the pulsed charge density is

$$\mathrm{d}^2\Phi/\mathrm{d}x^2 - (1/c^2)\mathrm{d}^2\Phi/\mathrm{d}t^2 = -Q(x,t)/\varepsilon_0\,, \tag{9}$$

where Φ and c are scalar potential and velocity of light, respectively. $Q(x,t) = -Q(t)\delta(x) + Q(t)\delta(x - 2a)$ with the effective charge separation distance, $2a$. The time variation of the dipolar polarization density of $P(t) = 2aQ(t)$ generates EM waves. The Poynting vector at the distance $R(R \gg 2a)$ using Eq. (8) is given as

$$N(x,t) = (1/4\pi R)^2(\mu_0/c)[\mathrm{d}^2P/\mathrm{d}t^2]^2\sin^2\theta = (1/4\pi R)^2(\mu_0/c)\sin^2\theta\{\alpha M_0 \times [\varepsilon\rho/(\tau - \varepsilon\rho)][\exp(-t/\tau)/\tau^2 - \exp(-t/\varepsilon\rho)/\varepsilon^2\rho^2]\}^2\,, \tag{10}$$

where θ is the angle between the direction of the dipole and the distance vector R. The electric (or magnetic) field, i.e. $(N(x,t))^{1/2}$, is reciprocally proportional to the distance R.

3.1.2. *Power spectrum and the decay time*

(a) Decay in the conductive earth crust

The wave vector k, for EM waves in a conductive earth is a complex number, i.e. $k = k' + ik''$ from Maxwell's equations, where the imaginary part k'' is, using the permeability μ,

$$k'' = \omega(\mu\varepsilon/2)^{1/2}[(1 + (1/\omega\varepsilon\rho)^2)^{1/2} - 1]^{1/2} . \tag{11}$$

The intensity decays as $\exp(-k'R)$ as shown in Fig. 3(a) at each distance $R = 10$ km and 100 km for EM waves at the frequency, $f(\omega = 2\pi f)$. Only EM waves at very low frequency (VLF) or ultra low frequency (ULF) levels propagate in the conductive earth crust.

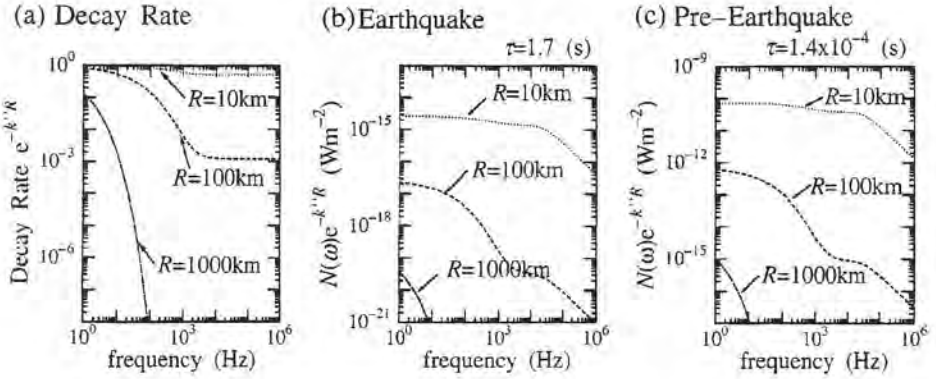

Fig. 3. (a) Decay of EM waves at a distance R as a function of the frequency due to the resistivity $\rho = 10^6$ Ωm in granite bedrocks. (b) Power spectra of EM waves due to the time-dependent seismic electric dipole at the time of an earthquake ($\tau = 1$ s). (c) local fractures prior to an earthquake for $\tau = 1.4 \times 10^{-4}$ s. Note that EM waves are produced as preseismic ones, more efficiently than coseismic ones.

(b) Another earth-waveguide of the earth crust as a dielectric slab

The parallel plate waveguide for the surfaces of the sea and ionosphere constitute an earth waveguide.[15] Seismic EM waves would also propagate through the earth's crust as a dielectric slab. We suggest another earth-waveguide consisting of the conductive Moho plane and the sea floor which allows the propagation of EM waves through long distances. The two earth-waveguides are coupled through island and land. The cut-off frequency, f_c, of the atmospheric waveguide is 2–3 kHz, while that of the Moho plane-Earth surface dielectric slab waveguide is 1.25 kHz for the specific dielectric constant $\varepsilon^* = 8$. The wavelength in the waveguide, λ_g, is

$$\lambda_g = (1/{\lambda_0}^2 - (1/2d)^2)^{-1/2} , \tag{12}$$

where λ_0 is the wavelength in the atmosphere ($\lambda_0 = c/f$) or in the dielectric earth ($\lambda_0 = c/f(\varepsilon^*)^{1/2}$) and d is the depth of the conductive plane.

3.1.3. *Theoretical basis of the VAN method: 1/R-dependence and selectivity*

The DC measurement of seismic electric signal (SES) known as the Greek VAN method[16] is in controversy over its alleged success in earthquake prediction.[17] Empirical formula used in the analysis of seismic electric signals (SES) by the VAN method indicate that the field intensity is proportional to $1/R$, suggesting the possibility of measuring the electric field of EM waves. The fact that they pick up only the signal whose intensity is proportional to the electrode separation might indicate the measurement of that long wavelength EM waves at ULF. The SES might come from the time averaged evanescent ULF waves rather than from the dipolar DC field proportional to $1/R^3$.

If the frequency is lower than f_c, the imaginary wavelength or wavevector ($k_g = 2\pi/\lambda_g$) leads to evanescent waves with an exponential decay in intensity which is nearly reciprocally proportional to the distance from the epicenter. Standing waves produce ripples in the intense electric field and might give the seismic electric field at a long distance from the epicenter, while no field is observed in between. A complex geography of island archipelagoes in Greece might be the reason for the "selectivity" of the VAN method considering our earth waveguide model. One can extend the model to the formation of stripe clouds asserted by amateurs as earthquake clouds though no meteorologists admit its presence. A standing wave produces an intense electric field and might ionize atmospheric molecules leading to the nucleus of cloud formation.

3.1.4. *The power spectrum and the estimated intensity of SES*

The Fourier transform of Eq. (10) gives a power spectrum having white noise and then $1/f$-dependence starting above either $1/\varepsilon\rho$ or $1/\tau$. However the power spectrum for $\rho = 10^6$ Ωm of granite depends strongly on $\exp(-k''R)$, as indicated in Figs. 3(b) and 3(c) at the distances $R = 10$ km, 100 km and 1000 km for $\tau = 1.7$ s at an earthquake and $\tau = 1.4 \times 10^{-4}$ s for local fractures, respectively.

Suppose $\alpha = 10^{-15}$ C/N and the moment magnitude $M_W = 6$ leading to $M_0 = 10^{18}$ Nm and $\alpha M_0 = 10^3$ Cm. The stress at the fault zone with the volume $2aA$ is changed by the preseismic movement in a short time τ. However, the stress change caused at the fracture source propagates at the speed of $\beta = 3.5$ km/s in a/β, i.e. in a few seconds. Hence, we must multiply τ and the power density as shown in Fig. 3(c). This leads to the energy flows at 1 Hz as 7×10^{-11} W/m^2 and 6×10^{-13} W/m^2 for preseismic energy at the distances 10 km and 100 km, respectively. Then, the field intensities are $F = (\mu c N)^{1/2} = 1 \times 10^{-4}$ V/m and 1×10^{-5} V/m, respectively. These are close to those reported in the SES measurement.[16,17] Presumably, the electric fields of ULF evanescent waves was measured by the VAN method.

3.2. *An early earthquake warning system using seismic electric signals (SES)*

3.2.1. *Preliminary measurement of pulsed electric field with a digital storagescope*

A preliminary attempt to measure seismic pulsed current as expected from this theory was made by immersing parallel plate electrodes in an aquarium as a dielectric antenna and measuring the induced pulse voltage with a digital storage oscilloscope (DSO:AD-5146, A&D Co.) as shown in Fig. 4. The frequency range of the DSO is from 10 Hz to 10 MHz. This system gives pulsed electric fields in a derivative form.

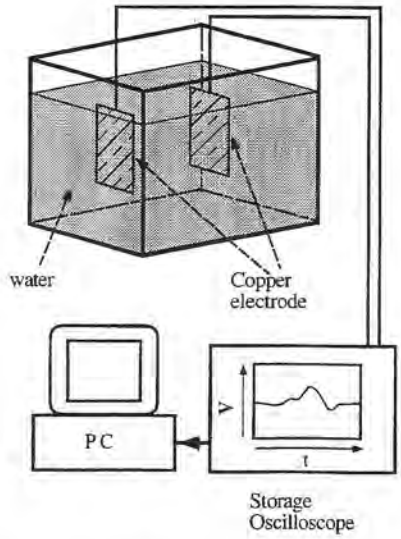

Fig. 4. A parallel-plate antenna in an aquarium for the preliminary measurements of electric pulses with a broad-band digital storage oscilloscope.

Figure 5(a) shows the last one of the five pulses measured at 14:47, 15:25, 16:03, 16:12 and 17:23 before an earthquake at 17:37 on May 29, 1996 (Magnitude 3.8, at the depth of 20 km and the ground distance of 15 km from the epicenter). No coseismic pulse was observed. No seismic wave was observed at the time of the pulses. Note that we are not attempting to predict the occurrence of the earthquake. It is unfortunately not clear whether these pulses are really related to the earthquake or not.

Figure 5(b) shows lightning observed on some other day. The intensity of 0.25 V/m is comparable to those which cause SAAB in sensitive aquatic animals ($> 0.1 - 1$ V/m)[3] and having orders of magnitude smaller than SES using the DC method (10^{-5} V/m). We also observed sudden anomalous movements of eels and hamsters simultaneously with the measurements of intense electric pulses of

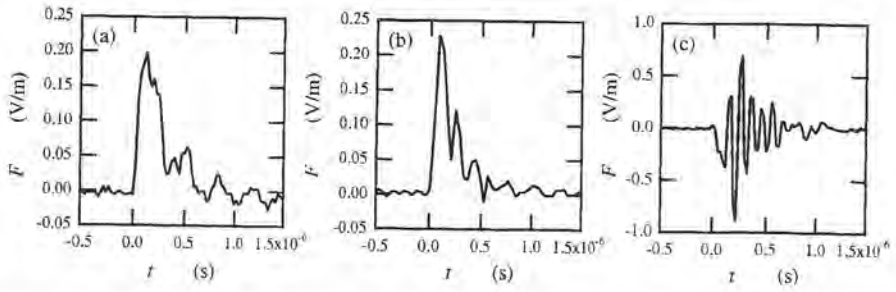

Fig. 5. Pulsed electric field measured (a) one hour prior to an earthquake of the magnitude 3.8. The correlation with the earthquake is not clear. (b) at the time of atmospheric lightning, and (c) noises by switching the power line on and off.

about 2 V/m. Although the correlation with the earthquake of magnitude 3.9 which occurred 2.3 days after this event is not clear, SAAB are behavioral responses to electric pulse stimuli similar to that observed during lightning.

Figure 5(c) represents the artificially induced noises caused by switching on and off the power line in the room. The pulse signal shape looks different from the natural ones. Noises may be distinguished more easily by pulses using DSO with a broad bandwidth rather than by VLF and ULF waves using a narrow bandwidth detector.

The pulses observed before an earthquake were all similar to that in lightning, exhibiting a sharp risetime of less than 0.1 ms. This may arise either from seismic signals related to fractures having short τ or from lightning induced between the seismic pulsed charges on the ground and clouds. A correlation between lightning and earthquakes from the observation of VLF[18] and ULF waves[4,5] might be ascribed to cloud-ground discharges caused by seismic ground charges though their interpretations are different.

3.2.2. *Early warning system rather than prediction*

Measurements of broad-band EM waves as pulses and the Fourier transform of pulse shapes may be made to study the frequency components. Parameters $M_0, \varepsilon\rho$ and τ can be deduced by detecting electric pulses from the on-site computer analysis of their shape, which will tell the nature of the seismic P- and S-waves well before the arrival of seismic waves. A new field of "*electroseismology*" may be developed using SES.

This paper does not make a claim for earthquake prediction using either the VAN method or pulsed field measurement. We are neither sure of the mechanism of the generation of seismic precursor EM waves nor its relation to the rock rupture at the hypocenter source nucleus. Provided that intense seismic electro-magnetic waves were generated before an earthquake, the precursor time[7] would still be a

statistical one. However, EM waves propagate at the speed of light, much faster than seismic waves.

4. Conclusion

EM behavior of a fault following a mathematical model used in seismology gives a formula to explain SES and EM anomalies. The sustaining charges at a fault zone are due to the generation of charges during the seismic stress changes by fault movements or by local fractures prior to an earthquake. The pulsed dipolar charge densities at a fault zone illustrate the emission of EM waves and the polarization of the ionosphere. Electric field pulses have actually been observed with a digital storage oscilloscope prior to an earthquake and during lightning. The SES detected earlier than seismic P-waves might be utilized as a primary signal using a new earthquake early warning system.

Acknowledgments

We thank Emeritus Profs. M. Date, R. Ueda, M. Kumazawa and Dr. C. Yamanaka for a discussion on piezoelectric effects of rocks, Prof. Sumitomo at the Research Center of Earthquake Prediction, Kyoto University, for supplying seismic wave data on May 29 1996, and Mr. H. Sasaoka for the valuable discussion.

Note Added in Proof – The area of a fault $A = 2ah$ is assumed, where h is the depth of a fault plane due to the structure of Earth. Then the earthquake moment is $M_o = \mu DA = \Delta\sigma(2a)^2 h \propto (2a)^2$ or $2a \propto M_o^{1/2}$. The power density of electric dipoles, np^2/τ, is given as $N \propto M_o^{1/2}$ using $\tau = (\Delta\sigma/\sigma_o)(a/\beta)$. The intensity of SES, ΔV is proportional to the electric field and so $N^{1/2}$ leading to $\Delta V \propto M_o^{1/4}$ A scaling law of $\log \Delta V = 0.375M + c$ is thus obtained theoretically using the definition of a moment magnitude $M_W = (\log M_o - 9.1)/1.5$ which coincides with the empirical one, $\log \Delta V = 0.37M + c$, in the VAN method.

References

1. K. Wadatsumi, *1591 Witnesses Phenomena Prior to Earthquake*, Tokyo Pub. Tokyo, 1995 (in Japanese).
2. M. Ikeya and S. Takaki, "Electromagnetic model of a fault for earthquake lightnings (EQLs)", *Jpn. J. Appl. Phys.* **35** (1996) L355–L357.
3. M. Ikeya, S. Takaki, and D. Takashimizu, "Electric shocks resulting in seismic animal anomalous behaviors (SAABs)", *J. Phys. Soc. Jpn.* **56** (1996) 710–712.
4. Y. Fujinawa and K. Takahashi, "Emission of electromagnetic radiation preceding the Ito seismic swarm of 1989", *Nature* **347** (1990) 376–378.
5. M. Hayakawa and Y. Fujinawa, eds., *Electromagnetic Phenomena Related to Earthquake Prediction*, Terra Scientific, Tokyo, 1994, p. 677.
6. C. H. Scholz, *The Mechanics of Earthquake and Faulting*, Cambridge Press, Cambridge, 1990, p. 439.
7. H. Kanamori and D. Anderson, "Theoretical basis of some empirical relations in seismology", *Bull. Seism. Soc. Am.* **65** (1975) 1073–1095.

8. J. M. Carlson, J. S. Langer, and B. E. Shaw, "Dynamics of earthquake faults", *Rev. Mod. Phys.* **66** (1994) 657–670.
9. M. Matsu'ura, in *Theory of Earthquake Premonitory and Fracture Processes*, ed. R. Teiseyre, Part I, Chap. 5, Polish Scientific Publisher, 1995.
10. D. A. Lockner, M. J. S. Johston, and J. D. Byerlee, "A mechanism to explain the generation of earthquake lights", *Nature* **302** (1983) 28–33.
11. K. Kumazawa, "Disturbances in electromagnetic field in rocks due to piezoelectric effects in connection with seismic waves", *J. Sci. Nagoya Univ.* **9** (1961) 54–79.
12. M. P. Volarovich and G. A. Sobolev, "Use of piezoelectric effects of rocks for subsurface exploration of piezoelectric media", *Dokl. Akad. Nauk. SSSR* **162** (1965) 11–13.
13. Y. Enomoto and H. Hashimoto, "Emission of charged particles from indentation fracture of rocks", *Nature* **346** (1990) 641–643.
14. M. Ikeya, "Electromagnetic phenomena and anomalous animal behaviors accompanying earthquake", *Kagaku* **66** (1996) 408–418 (in Japanese).
15. O. A. Molchanov, M. Hayakawa, and V. A. Rafalsky, "Penetration of electromagnetic emissions from an underground seismic source into atmosphere, ionosphere and magnetosphere" in *Electromagnetic Phenomena Related to Earthquake Prediction*, eds. M. Hayakawa and Y. Fujinawa, Terra Scientific, Tokyo, 1994, pp. 565–605.
16. P. Varatos and K. Alexopoulos, "Physical properties of the variations of the electric field of the Earth preceding earthquakes", *Tectonophysics* **110** (1984) 73–98.
17. R. J. Geller, "VAN: a critical evaluation" in *A Critical Review of VAN*, ed. J. Lighthill, World Scientific, Singapore, 1996, 155–238.
18. K. Oike and T. Yamada, "Relation between shallow earthquakes and electromagnetic noises in the LF and VLF ranges" in *Electromagnetic Phenomena Related to Earthquake Prediction*, eds. M. Hayakawa and Y. Fujinawa, Terra Scientific, Tokyo, 1994, pp. 115–130.